Characterization of a Novel Ni/Activated Carbon-TiO₂ Composites and Photocatalystic Mechanism Derived from Organic Dye Decomposition

LEI ZHU, JUNG-HWAN CHO, ZE-DA MENG, JONG-GEUN CHOI, CHONG-YEON PARK, TRISHA GHOSH and WON-CHUN OH[*]

Department of Advanced Materials Science & Engineering, Hanseo University, Chungnam 356-706, South Korea

*Corresponding author: Fax: +82 41 6883352; Tel: +82 41 6601337; E-mail: we_oh@hanseo.ac.kr

The activated carbon (AC) modified with different concentration of nickel chloride to prepare Ni coated activated carbon and it was employed for preparation of Ni/activated carbon-supported TiO₂ composite photocatalysts with titanium(IV)-*n*-butoxide. The characterizations of Ni/ activated carbon-supported TiO₂ composite photocatalysts were determined by employing BET, SEM, XRD and EDX instruments to analyze the potential factors. The photocatlytic activity was evaluated by degradation of methyl blue and methyl orange dye. The results demonstrated that as-prepared samples could effectively photodegrade methylene blue and methyl orange under UV irradiation. When the optimal nickel dosage was 7.95 wt % its photo-decolorization efficiency was achieved the highest photodegradation rate in this study.

Key Words: Photo-Fenton, Ni/activated carbon-supported TiO₂, Methyl blue, Methyl orange.

INTRODUCTION

Titanium dioxide (TiO₂) has been widely used as a photocatalyst for solar energy conversion and environmental applications (water and air purification) because of good photoactivity, high chemical stability, low cost and nontoxicity. When TiO₂ is irradiated by light with wavelength (λ) < 387 nm, electrons are promoted across the band gap (3.2 or 3.0 eV in the anatase or rutile crystalline phase, respectively) into the conduction band, leaving holes in the valence band[1]. These holes have high oxidation power, then react with adsorbed hydroxide ions to produce hydroxyl radicals, the main oxidizing species responsible for the photooxidation of organic compounds. However, the application of pure TiO₂ is limited, because it requires UV activation. With pure TiO₂, only < 5 % of the solar radiation reaching the earth's surface can be used.

Researchers have discovered that during the photo-degradation process, interaction by certain pollutant molecules or their intermediates could cause the titania to coagulate, thereby reducing the amount of UV radiation from reaching the titania active centers (due to reduction of its surface area) and thus reducing its catalytic effectiveness. In order to overcome this coagulation problem, some researchers have used different materials as a support for the titania photocatalyst[2,3]. Various substrates have been used as a catalyst support for the photocatalytic degradation of polluted water. For example glass materials: glass beads[4], glass reactors[5], microporous cellulosic

membranes[6], ceramic membranes[7], zeolites[8] and stainless steel[9] were used as a support for titania.

Several attempts have been adopted to enhance the photocatalytic performance of TiO₂, such as immobilization of TiO₂ powder onto supports like activated carbon fiber (ACF)[10] and activated carbon (AC)[11-13]. Activated carbon is highly adsorptive owing to its developed pore structure and high specific area; moreover the particle size of commercial activated carbon is usually in the micro-scale range. Activated carbon must be of medium surface area and porosity, to facilitate the diffusion of pollutants and release of products from the surface and so many authors have reported a synergistic effect for activated carbon-supported TiO₂ systems[11-13], such a high photocatalytic activity, photosensitivity and high adsorptive ability. Activated carbon increases the photodegradation rate by progressively allowing an increased quantity of substrate to come in contact with the titania through means of adsorption. This is important because it has been established that the oxidizing species (OH•) generated by the photocatalyst, does not migrate very far from the active centers of the titania and therefore degradation takes place on the catalyst surface. The adsorption of pollutant to be then transfer by a common interface from activated carbon to TiO₂ it was firstly pointed out by Matos *et al.*[14].

In another aspect of improving photocatalytic activity, reducing the recombination of holes and electrons by doping TiO₂ with transition metals was proposed the most common method. Also, the effects of some transition metal ion dopants

such as Fe, V, Mn, Co and Ni have been investigated for the TiO$_2$ system[15]. On the other hand, Ni^{2+} has been found to be an efficient dopant for improving the photocatalytic activity of certain semiconductor photocatalysts for hydrogen evolution from water[16,17]. The reason for this enhancement is still far from satisfactory explanation. Jing et al.[18] reported the synthesis of Ni doped mesoporous TiO$_2$ and its photocatalytic activity for hydrogen evolution in aqueous methanol solution. It was found that Ni^{2+} doping played an important role in improving the thermal stability and controlling the morphology of the meso-porous photocatalyst. More importantly, existence of Ni^{2+} greatly suppressed recombination of electron-hole pairs on the surface of the meso porous photocatalyst, hence enhancing its activity[18].

More recently, the simultaneous doping of two kinds of atoms into TiO$_2$ has attracted considerable interest, since it could result in a higher photocatalytic activity and peculiar characteristics compared with single element doping into TiO$_2$. Some studies were reported on co-doped materials such as C and N[19], S and N[20], B and N[21] and N and a variety of metal ions[22,23] and in some cases authors underlined the synergistic effect of co-doping. For example, Cong et al.[24] reported that co-operation of nitrogen and iron cations led to the much narrowing of the band gap and greatly improved the photo-catalytic activity in visible light region. Klabunde and co-workers[25] synthesized C-doped and C and V co-doped TiO$_2$ photocatalysts that were quite active for the degradation of acetaldehyde. Tryba et al.[26] prepared TiO$_2$ modified by carbon and iron photocatalyst by impregnating the powder TiO$_2$ with FeC$_2$O$_4$ solution and heating it at 400-800 ºC under flow of Ar gas. They reported that the Fe-C-TiO$_2$ sample showed the higher photoactivity for phenol decomposition and dyes degra-dation under UV light and H$_2$O$_2$. However, to our best knowledge, active carbon and nickel iron co-modified TiO$_2$ using sol-gel process followed with solvothermal method under moderate conditions have not yet been reported.

In the present paper, active carbon and nickel iron modified TiO$_2$ photocatalysts with enhanced photocatalytic activity for photodegradation of methylene blue (MB) and methyl orange (MO) under UV light were obtained directly via the combination of sol-gel process and solvothermal treatment at low temperature. The resulting composite photocatalysts were investigated using X-ray diffraction (XRD), scanning electron microscopy (SEM) and energy dispersive X-ray spectroscopy (EDX), BET surface area analysis. The effect of amount of nickel cations dopants on the properties of activated carbon modified TiO$_2$ was also investigated.

EXPERIMENTAL

Synthesis of nickel cations coated activated carbon composites: All solutions were prepared from deionized water (Milli-Q) and all reagents in the present work were of analytical grade and used as received. Commercially available activated carbon powders were used as adsorbent substrates, which were produced by the vapour activation of coconut shell as follows: some amount of coconut shell was pre-carbonized first at 773 K and then activated by steam diluted with nitrogen in a cylindrical quartz tube at 1023 K for 0.5 min. The obtained activated carbon was washed with deionized water and dried overnight in a vacuum drier at 683 K.

Nickel iron coated activated carbon composites were prepared through the adsorption of nickel cations (Ni^{2+}) in the presence of activated carbon in aqueous solution. A typical synthesis is as follows: activated carbon powder (5 g) was dispersed by sonication in 50 mL of deionized water. On the other hand, NiCl$_2$ (0.5, 1.0 and 1.5 mol) were dissolved in 10 mL of deionized, separately. Then the solution of activated carbon and the solution were mixed and stirred for 5 h at 333 K, separately. The obtained black precipitate was filtered, washed with deionized water and alcohol and dried in a vacuum at 373 K for 10 h.

Synthesis of Ni/AC-supported TiO$_2$ composites photo-catalyst: The Ni/AC-supported TiO$_2$ composites were fabri-cated via a sol-gel method and thermal annealing. 10 mL of titanium(IV) n-butoxide (TNB, C$_{16}$H$_{36}$O$_4$Ti, Acros Organics, USA) was dissolved into 80 mL benzene (99.5 %, ACS reagent, Korea) to form the solution A. 5 g of as-prapared Ni/AC powder was added to the solution A at 333 K under stirring for 5 h. After stirring and vaporizing for 2 h, the samples were filtrated and dried at 373 K for 8 h and then calcinated at 773 K for 1 h and the Ni/AC-supported TiO$_2$ composites photocatalysts were obtained.

Catalyst characterization: Crystallographic structure of the composites photocatalysts were obtained by XRD (Shimatz XD-D1, Japan) at room temperature with CuK$_\alpha$ radiation (λ = 0.154056 nm) and a graphite monochromator, operated at 40 KV and 30 mA. The EDX spectra were also used for elemental analysis of the samples. The morphologies of the photocatalysts were analyzed by SEM (JSM-5200 JOEL, Japan) at 3.0 keV, which was equipped with an energy dispersive analysis system of X-ray analysis (EDX). Nitrogen adsorption isotherms were obtained using a BEL Sorp analyzer (BEL, Japan) at 77 K. The BET surface area was calculated from these isotherms. The pore size distribution was calculated by BJH method. The UV-VIS spectra for the dye solution degraded by TiO$_2$, Ni/AC-supported TiO$_2$ photocatalysts under UV light irra-diation were recorded using a Genspec III (Hitachi, Japan) spectrometer.

Photocatalytic activity test: The photocatalytic activities of samples were evaluated in terms of the degradation of methylene blue (C$_{16}$H$_{18}$N$_3$SCl·3H$_2$O, Duksan Korea) and methyl orange (C$_{14}$H$_{14}$N$_3$NaO$_3$S, Duksan Korea) decompo-sition in aqueous solution under UV light illumination. The molecular structure and λ_{max} of organic dyes are shown in Table-1. The photodegradation reactions were carried out with a homemade photoreactor. A 20W UV lamp equipped with a UV cut-off filters (λ > 365 nm) was used as a UV light source. The distance between the light and the reaction tube was fixed at 100 mm. The initial concentration of methylene blue and methyl orange (c$_0$) was 1.0×10^{-5} mol/L. The photocatalyst powder (0.03 g) was dispersed in a 100 mL glass photoreactor containing 50 mL of dye solution. The mixture was sonicated for 10 min and stirred for 0.5 h in the dark in order to reach the adsorption-desorption equilibrium. At the given time in-tervals the sample of 3.5 mL was taken from the mixture and immediately centrifuged to remove the dispersed photocatalysts. The concentration of the clean transparent solution was analyzed by checking the absorbance at 665 nm[27] for methylene blue and 467 nm[28] for methyl orange with the UV-VIS spectro-photometer.

TABLE-1
MOLECULAR STRUCTURE AND λ_{max} OF ORGANIC DYES

Organic dyes	Molecular structure	λ_{max}
Methylene blue (MB)		665 nm
Methyl orange (MO)		465 nm
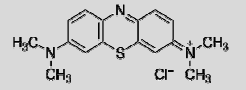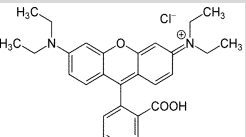
RESULTS AND DISCUSSION

Crystal structure and elemental analysis: Phase identification was carried out by XRD. Solid lines in Fig. 1 show XRD patterns of activated carbon supported TiO_2 and Ni/AC supported TiO_2 calcinated at 773 K for 1 h. The dashed line is the smoothed XRD pattern of activated carbon. In case of the activated carbon, very broad peaks at *ca.* 24.3 and 43.8º could be assigned to (0 0 2) and (1 0) of graphite[29]. The XRD patterns of activated carbon supported TiO_2 show the appearance of peaks at 2 h value of 25.4º, 38º, 49º, 55º, 63º corresponding to the (1 0 1), (0 0 4), (2 0 0), (2 1 1) and (2 0 1) planes of anatase type[30] matching with JCPDS No. 21-1272. No other peaks corresponding to rutile or brookite are observed. These planes confirm that the formed phase of TiO_2 in activated carbon matrix on the whole would be an efficient catalyst as it is believed that anatase phase is more catalytically active[31,32]. The X-ray analysis also suggests that the heat treatment of 773 K is sufficient to induce the anatase phase TiO_2 in the carbon structure. In case of samples containing nickel cations, significant characteristic peaks at 2 h = 44.5, 52.9 and 76.4[33] for nickel were detected. It is also evidently seen that the intensity of nickel peaks increase with an increase of $NiCl_2$ concentration.
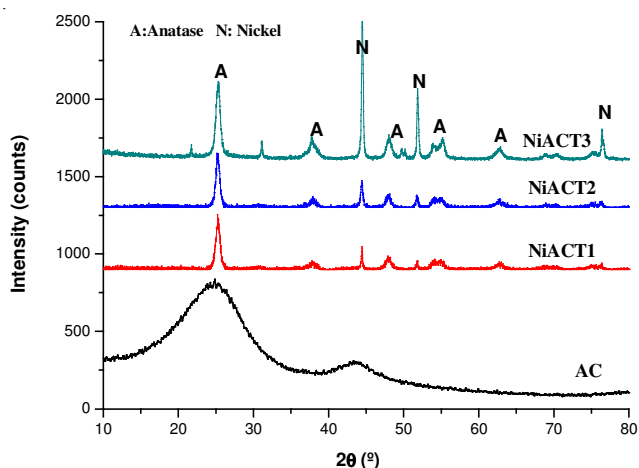
Fig. 1.   XRD patterns of Ni/AC-supported TiO_2-composites prepared by using different concentration of $NiCl_2$

EDX is carried out to probe composition and element weight per cent of the attached nanoparticles. The spectrum is shown in Fig. 2 for Ni/AC-supported TiO_2 composites. The data of EDX analyses of the Ni/AC-supported TiO_2 composites were listed in Table-2. These spectra showed the main elements as presence of C, O and Ni with strong Ti peaks. C, Ni and Ti
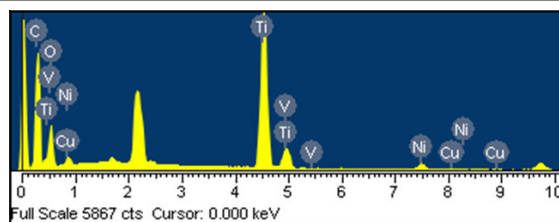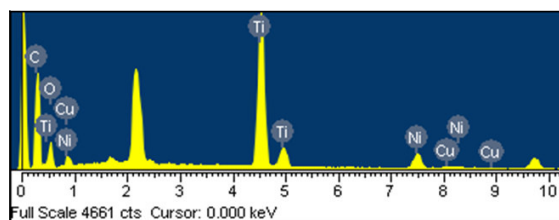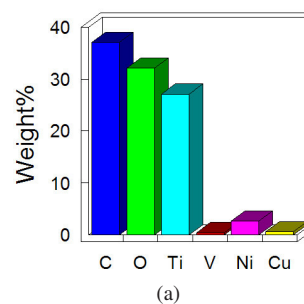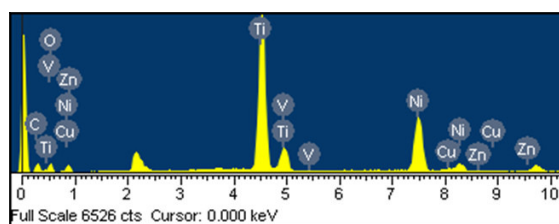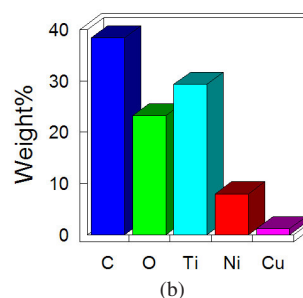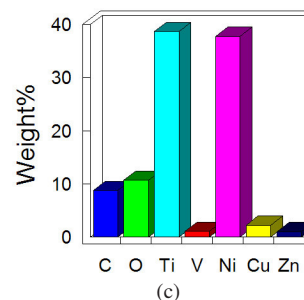
Fig. 2.   EDX microanalysis and element weight percentage of Ni/AC-supported TiO_2 composites: NiACT1 (a), NiACT2 (b), NiACT3(c)

TABLE-2
EDX ELEMENTAL MICROANALYSIS (wt. %) of Ni/AC-
SUPPORTED TiO₂ COMPOSITES PREPARED BY USING
DIFFERENT CONCENTRATION OF NiCl₂

Samples	Elements				
	C	O	Ti	Ni	Others
NiACT1	37.13	32.14	27.17	2.62	0.57
NiACT2	38.36	23.17	29.31	7.95	1.20
NiACT3	8.75	10.64	38.63	37.38	4.20

were confirmed as componental elements in most of the Ni/AC-supported TiO₂ composites. These results were presented the spectra corresponding to almost all samples decreased in C elements and increased in O, Ni and Ti elements.

BET surface area and pore properties measurements: N₂ nitrogen adsorption isotherms and pore size distributions of Ni/AC-supported TiO₂ composites were shown in Figs. 3 and 4. The BET surface area, pore volumes and average pore diameters are also listed in Table-3. All the Ni/AC-supported TiO₂ composites gave type I isotherms characterized by plateau that is nearly horizontal to the p/p₀ axis in the middle region with increasing of adsorbed volume in low relative pressure region. The specific surface area of the photocatalysts was gradually decreased by increasing the nickel contents treated in Ni/AC-supported TiO₂ composites suggests that the deposited nickel and TiO₂ particles could block the activated carbon pores. Generally, the BET surface area is considered to be decreased due to the blocking of the micropores by surface complexes introduced through the formation of the Ni/AC-supported TiO₂ composites. However, from pore volume and average pore diameters, it can be seen that the pore diameter is decreased a lot and it indicated that Ni compounds and TiO₂ particles agglomerated on the outside surface and on the inside surface of activated carbon. All of surface textural parameters for these composites were a considerably more decrease due to the pore structural transformation by nickel and titanium complexes on the activated carbon surface. The high distribution centers at 4.05, 3.55 and 3.12 nm can be attributed to NiACT1, NiACT2 and NiACT3, while the pore diameters are obviously reduced with increasing the concentration of nickel.

Fig. 4. Pore size distributions for the Ni/AC-supported TiO₂ composites

TABLE-3
TEXTURAL PROPERTIES OF Ni/AC-
SUPPORTED TiO₂ COMPOSITES

Samples	Parameter		
	S_{BET} (m²/g)	Micropore volume (m³/g)	Average pore diameter (nm)
NiACT1	247	0.1343	3.9576
NiACT2	236	0.1334	3.3776
NiACT3	93	0.0763	3.3174

TiO₂ composites were characterized by SEM in Fig. 5. It can be observed that the prepared composite mainly consists of shaped particles and have a high tendency to agglomerate. However, it is observed that the activated carbon has much pore structure and the nickel and TiO₂ particles are blocked into the pore of activated carbon or coated on the activated carbon, which was consistent with the N₂ adsorption experiment. In comparison of different concentrations of nickel and TiO₂ particles on activated carbon surface, there was no significant difference. It can be attributed that when the crystal particle size is very small, it can easily agglomerate due to the weak forces of the surface.

Fig. 3.   Nitrogen adsorption isotherms obtained from the Ni/AC-supported TiO₂ composites

Morphology and structure analysis: The typical micro-surface structures and morphology of the Ni/AC-supported
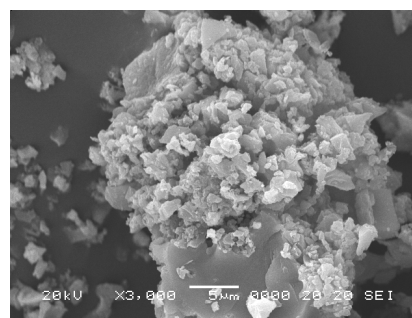
(a)
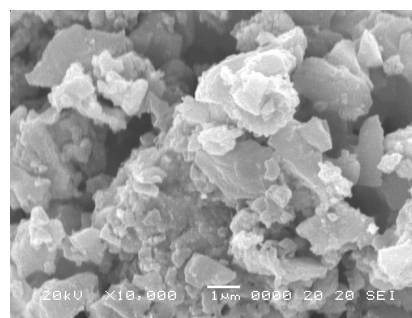
(b)
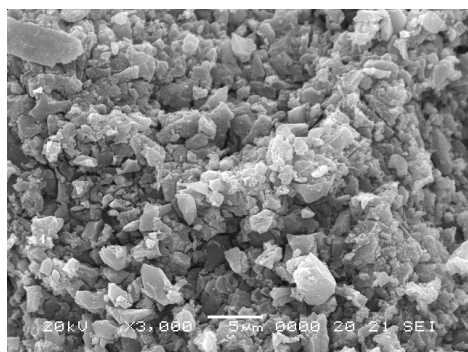
(c)
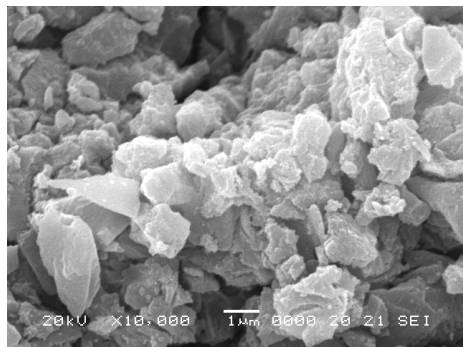
(d)
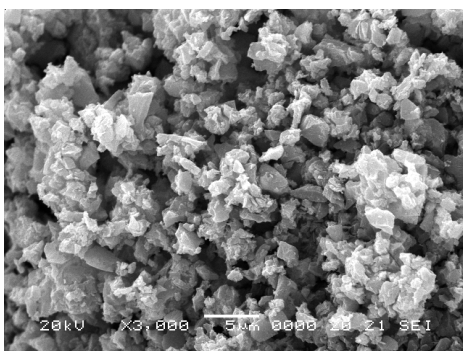
(e)
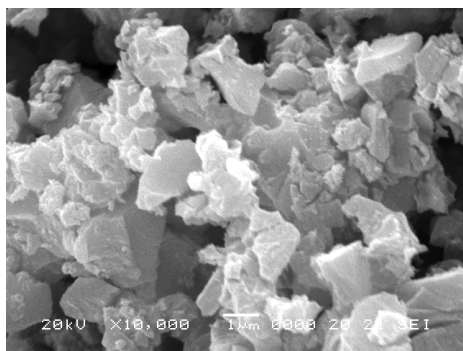
(f)

Fig. 5. SEM images of Ni/AC-supported TiO$_2$ composites prepared by using different concentration of NiCl$_2$; (a) and (b) NiACT1, (c) and (d) NiACT2, and (e) and (f) NiACT3

Photocatalytic activity: Photodegradation of methylene blue and methyl orange organic dye solution under UV light irradiation is employed to evaluate the photocatalytic activity of the prepared catalysts. Initially, control tests on degradation of dye solution (*ca*. 1×10^{-5} mol/L) were carried out in specified

conditions described below: the data are obtained following a two step experiments. The first step is placed in dark to adsorb dye and the second step is exposed to UV light to degrade dye solution. Fig. 6 shows the relative absorbance of methylene blue and methyl orange in the aqueous solution on time under irradiation of UV light for Ni/AC-supported TiO$_2$ composites and the concentrations of methylene blue and methyl orange solution decreased regularly with an increase of irradiation time for all of samples. It is worth to note that the surface area of NiACT3 is much lower than NiACT1 and NiACT2, so its adsorptive property is lower than other samples at our experiment condition. As mentioned at experiment, when the samples irradiated under UV lamp by an order of 30, 60, 90 and 120 min, the NiACT2 sample produced significantly higher efficiency of methylene blue and methyl orange. With increasing the content of Ni^{2+}, the photocatalytic efficiency was not correspond to the increase. The NiACT2 sample with Ni content of 7.95 wt % shown the best photocatalytic decolorization ability of methylene blue and methyl orange solution, it can be considered that using a larger amount of Ni^{2+} as dopant, on the contrary the Ni^{2+} was easy to be the recombination center of electron-hole pairs which results that decrease the photocatalytic efficiency. On the other hand, as shown in Table-1, for methylene blue molecules, which have obverse tropism (1.43 nm × 0.61 nm), end tropism (1.43 nm × 0.4 nm) and side tropism (0.61 nm × 0.4 nm), its width and height were larger than that of methyl orange, it can be found methyl orange were decomposed at a higher degree than that of methylene blue, as shown with the curves of degradation.
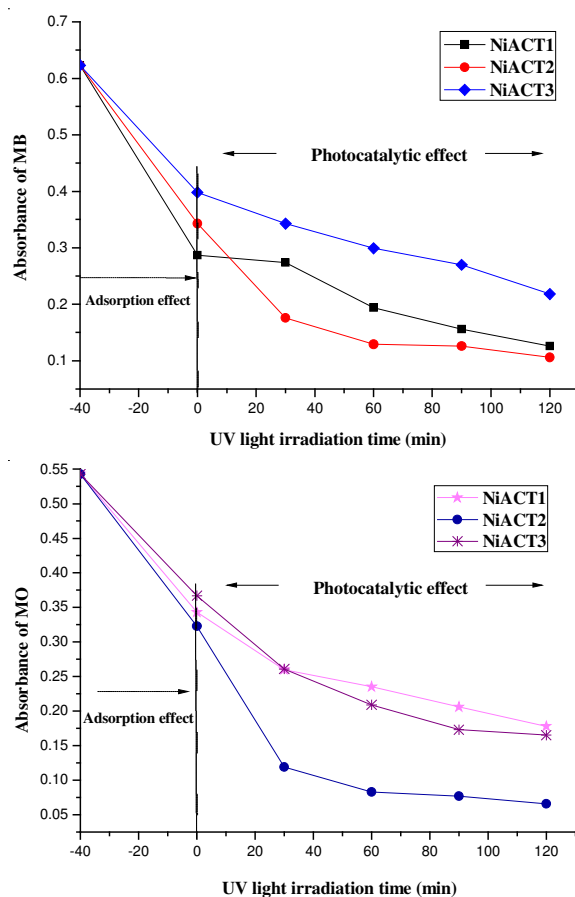
Fig. 6. Relative concentration of the methylene blue and methyl orange solution degraded by different samples after UV light irradiation

During the photo degradation process, suitable adsorption capacity is crucial for high photocatalytic activity. An important step in the photocatalytic process is the adsorption of reacting substances onto the surface of the catalyst. Activated carbon has a well-developed pore structure, very large surface area and strong adsorption capacity and is widely used as an adsorbent and catalyst support. It is considered that the activated carbon component absorbed the dye solution and then the TiO_2 component degrades due to a photocatalytic reaction.

Reactivity of TiO_2 depends on many factors: the adsorption of dye on catalyst surface, band-gap energy, surface area, crystal size, crystallinity and electron-hole recombination rate, therefore an explanation of reactivity order is complicated. The addition of nickel cation on the nanocrystalline TiO_2 photocatalyst surface can enhance the photocatalytic degradation activity due to the lower crystal size, higher surface area, higher efficiency for the electron hole regeneration and the charge trapping. The charge trapping can be demonstrated by the following equations:

$$Ni^{2+} + h\nu \rightarrow Ni^{2+}(e^-) + Ni^{2+}(h^+) \tag{1}$$

$$TiO_2 + h\nu \rightarrow TiO_2(e^-) + TiO_2(h^+) \tag{2}$$

$$Ni^{2+}(e^-) + O_2 \rightarrow Ni^{2+} + O_2^{\bullet-} \tag{3}$$

$$TiO_2(e^-) + O_2 \rightarrow TiO_2 + O_2^{\bullet-} \tag{4}$$

$$Ni^{2+}(h^+) + H_2O \rightarrow Ni^{2+} + OH^\bullet + H^+ \tag{5}$$

$$TiO_2(h^+) + H_2O \rightarrow TiO_2 + OH^\bullet + H^+ \tag{6}$$

$$O_2^{\bullet-} \text{ or } OH^\bullet + \text{methylene blue} \rightarrow \text{degradation products} \tag{7}$$
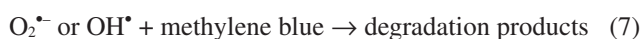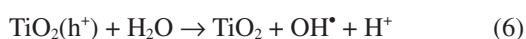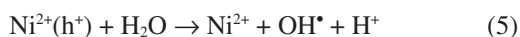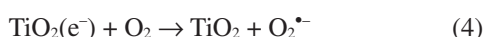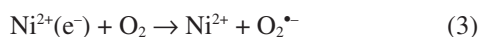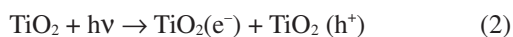
The photocatalytic reaction is initiated by the absorption of UV-light photons. Local excitation of the $NiCl_2$ by UV light affords charge transfer-ligand-to-metal. The labile nickel intermediate will rapidly transfer an electron to the conduction band of C-TiO_2, while the chlorine atom abstracts an electron from the oxygen lattice. At the same time, UV light irradiation of C-TiO_2 results in the creation of photogenerated holes in its valence band and electrons in its conduction band. Conduction band-electrons from both C-TiO_2 and $NiCl_2$ can easily transfer to the metal Ni through the Schottky barrier. In this way, the photogenerated electrons and holes are efficiently separated. At the same time, the modified composites by metal can enhance the photocatalytic activity greatly and show the practical benefits for industrial application.

The valence band-holes in C-TiO_2 and electrons trapped by metal Ni react with OH⁻ and molecule O_2 on the catalyst surface to form $OH^\bullet$ radicals and $O_2^{\bullet-}$ superoxide anion radicals, respectively. The photogenerated hole-based oxidation is thought to play an important role in photocatalytic reaction. The $O_2^{\bullet-}$ radicals then interact with adsorbed H_2O to produce more $OH^\bullet$ radicals, which are known to be the most oxidizing species for the degradation of organic compounds. The nickel effect on accelerating the photocatalytic ability is due to a photo-Fenton process. In photo-Fenton reactions, the process of metal oxidation and reduction occur after each other, giving rise to $OH^\bullet$ radicals, which are known to be responsible for the degradation of organic compounds. When transition metal ions replaced Ti ions of TiO_2, most of the dopant levels appeared between the valence band and the conduction band of TiO_2, which can increase the surface trapping rate of carrier and

retarded the electron-hole recombination. A simple schematic mechanism of the photocatalytic activity of Ni/AC-supported TiO_2 composites is shown in Fig. 7.
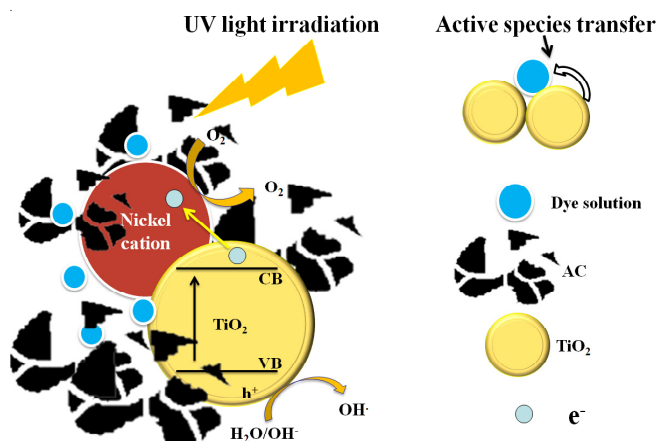
Fig. 7.   Reaction mechanism of the Ni/AC-supported TiO_2 composite under UV light irradiation

Conclusion

The activated carbon modified by different concentration of nickel chloride and then reacted with TNB to prepare Ni/AC-supported TiO_2 composites by sol-gel method. The data of the textural surface properties revealed that there is a slight decrease in the BET surface area and pore size of composites. N_2 adsorption data showed that the composites had decreased surface area compared with the pristine activated carbon. EDX results showed the presence of C, O and Ti with Ni element in the Ni/AC-supported TiO_2 composites. Furthermore, the adsorption effect and the photocatalytic effect were confirmed by the decomposition processes for the organic dyes solution (methylene blue and methyl orange). Especially efficient is the charge separation in the case of the Ni/AC-supported TiO_2 composites photocatalyst during irradiation with UV light, when the optimal nickel dosage was 7.95 wt % its photo-decolorization efficiency was achieved the highest photodegradation rate in this study.

REFERENCES

1. X. Chen and S.S. Mao, *Chem. Rev.*, **107**, 2891 (2007).
2. G.L. Puma, A. Bono, D. Krishnaiah and J.G. Collin, *J. Hazard. Mater.*, **157**, 209 (2008).
3. K.E. O'Shea, E. Pernas and J. Saiers, *Langmuir*, **15**, 2071 (1999).
4. N. Serpone, E. Borgarello, R. Harris, P. Cahill and M. Borgarello, *Sol. Energy Mater.*, **14**, 121 (1986).
5. J. Sabate, M.A. Anderson, H. Kikkawa, M. Edwards and C.G. Hill, *J. Catal.*, **127**, 167 (1991).
6. I.R. Bellobono, B. Barni and F. Gianturco, *J. Membr. Sci.*, **102**, 139 (1995).
7. Y.J. Zhao, W.H. Xing, N.P. Xu and F.-S. Wong, *J. Membr. Sci.*, **254**, 81 (2005).
8. Y. Xu and H. Langford, *J. Phys. Chem.*, **99**, 11501 (1995).
9. Y.M. Gao, H.S. Shen, K. Dwight and A.Wold, *Mater. Res. Bull.*, **27**, 1023 (1992).
10. W.C. Oh and M.L. Chen, *J. Ceram. Proc. Res.*, **9**, 100 (2008).
11. J. Arana and J.M. Dona, *Appl. Catal. B: Environ.*, **44**, 161 (2003).
12. S.X. Liu, X.Y. Chen and X. Chen, *J. Hazard. Mater.*, **143**, 257 (2007).
13. M.L. Chen, F.J. Zhang, Z.D. Meng, K. Zhang and W.C. Oh, *J. Photocal. Sci.*, **1**, 19 (2010).
14. W.C. Oh and F.J. Zhang, *J. Photocal. Sci.*, **1**, 63 (2010).

16. A. Kudo and M. Sekizawa, *Chem. Commun.*, **15**, 1371 (2000).
17. T. Sreethawong, Y. Suzuki and S. Yoshikawa, *Int. J. Hydrogen Energ.*, **30**, 1053 (2005).
18. D.W. Jing, Y.J. Zhang and L.J. Guo, *Chem. Phys. Lett.*, **415**, 74 (2005).
19. S. Yin, M. Komatsu, Q.W. Zhang, F. Saito and T. Sato, *J. Mater. Sci.*, **42**, 2399 (2007).
20. J.H. Xu, J.X. Li, W.L. Dai, Y. Cao, H.X. Li and K.N. Fan, *Appl. Catal. B: Environ.*, **79**, 72 (2008).
21. S. In, A. Orlov, R. Berg, F. Garci ́a, P.J. Sergio, M.S. Tikhov, S.W. Dominic and R.M. Lambert, *J. Am. Chem. Soc.*, **129**, 13790 (2007).
22. Y. Cong, J.L. Zhang, F. Chen, M. Anpo and D. He, *J. Phys. Chem. C*, **111**, 10618 (2007).
23. H. Wei, Y. Wu, N. Lun and F. Zhao, *J. Mater. Sci.*, **39**, 1305 (2004).
24. H. Sun, Y. Bai, Y. Cheng, W. Jin and N. Xu, *Ind. Eng. Chem. Res.*, **45**, 4971 (2006).
25. X.X. Yang, C. Cao, K. Hohn, L. Erickson, R. Maghirang, D. Hamal and K. Klabunde, *J. Catal.*, **252**, 296 (2007).
26. L. Zhu, Z.D. Meng, M.L. Chen, F.J. Zhang, J.G. Choi, J.Y. Park and W.C. Oh, *J. Photocal. Sci.*, **1**, 69 (2010).
27. L. Zhu, Z.D. Meng and W.C. Oh, *Chin. J. Catal.*, **32**, 926 (2011).
28. L.P. Zhu, G.H. Liao, W.Y. Huang, L.L. Ma, Y. Yang, Y. Yu and S.Y. Fu, *Mater. Sci. Eng. B*, **163**, 194 (2009).
29. Z. Zhu, A. Li, S. Zhong, F. Liu and Q. Zhang, *J. Appl. Polym. Sci.*, **109**, 1692 (2008).
30. Y. Ao, J. Xu, D. Fu, X. Shen and C. Yuan, *Colloids Surf. A*, **312**, 125 (2008).
31. Y. Gao and H. Liu, *Mater. Chem. Phys.*, **92**, 604 (2005).
32. A. Fujishima, T.N. Rao and D.A. Tryk, *Photochem. Photobiol.*, **C1**, 1 (2000).
33. J.-S. Jung, W.-S. Chae, R.A. McIntyre, C.T. Seip, J.B. Wiley and C.J. O'Connor, *Mater. Res. Bull.*, **34**, 1353 (1999).